Deep Chlorophyll Maximum Modelling in the Arctic Ocean Using a 1-D NPD Model

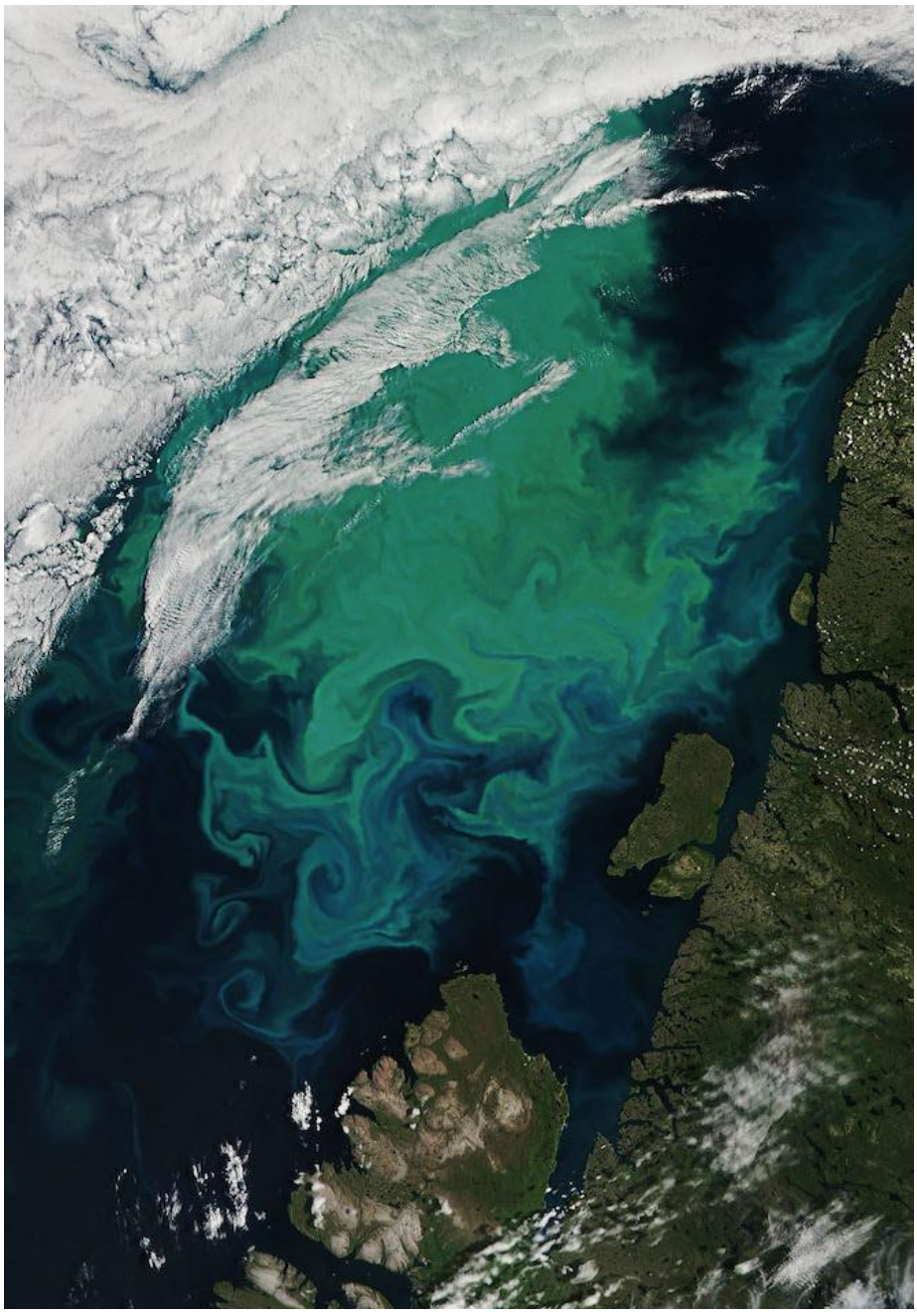

Student: Giacomo Gardella

Student ID: 223165

1. Introduction

Oligotrophic oceanic ecosystems often present subsurface maxima of primary production which are referred to as Deep Chlorophyll Maxima (DCM). The mechanisms underlying these phenomena are primarily the nutrient depletion in the surface layer and the self-shading of phytoplankton. When nutrients are poorly mixed into the surface layer, where most of the light is able to penetrate, they are rapidly depleted due to high primary production, leading to a downwards movement of the nutricline. Phytoplankton, which depend on nutrients for their growth, will follow this shift in nutrient concentration. As they move deeper into the water column, they get increasingly limited by light, which gets absorbed by the suspended particulate organic matter, the seawater, and the phytoplankton themselves. At a certain point, light becomes the factor limiting phytoplankton growth. At this upper boundary of the nutricline, high primary production hotspots are often observed during the summer (Beckmann and Hence, 2007).

The aim of this study is to create a simple one-dimensional NPD model that describes the seasonal formation of the deep chlorophyll maximum in an oligotrophic Arctic Ocean. The model results will be critically analysed based on the grit sensitivity and convergence. The relevance of selected model parameters, notably the diffusivity coefficient D_v, the remineralization rate, , the initial slope of the PI-curve, , and the half saturation constant for the nutrients HN, will be discussed.

2. Methods

2.1 Structure of the 1-D NPD model

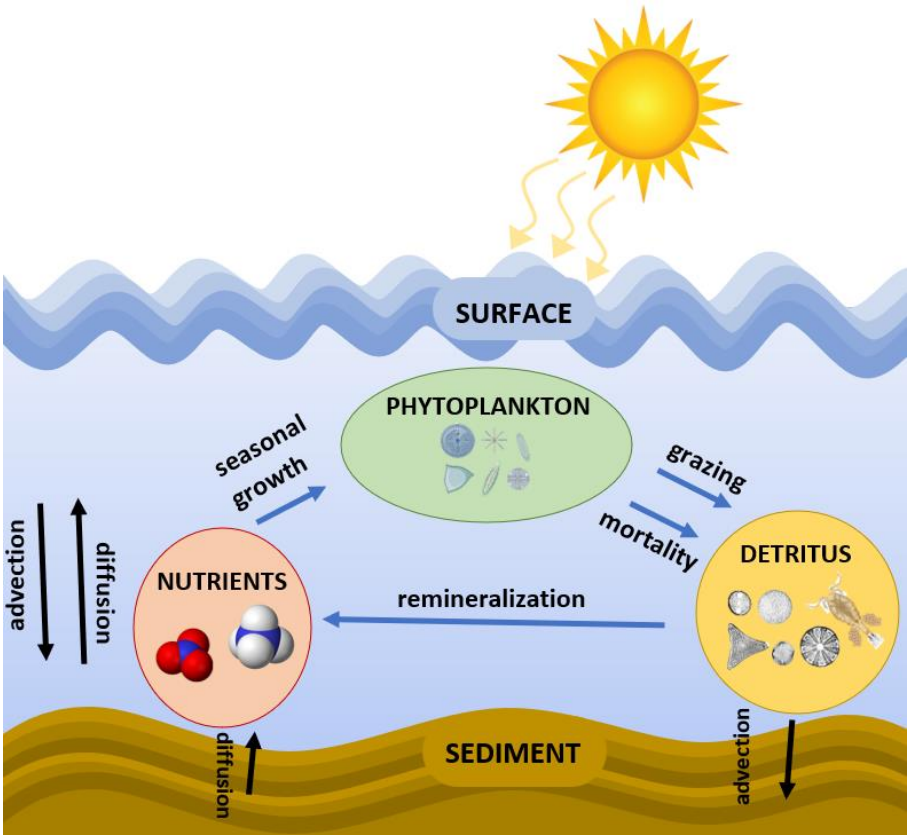

Figure 1: NPD model schematic.

The model used in this study is a one-dimensional Nutrient Phytoplankton Detritus (NPD) model. The three state variable are functions of both depth, *z*, and time, *t*, and defined in mmol of nitrogen (mmol N m^{-3}). Each state variable is subjected to both physical processes related to the hydrodynamics of the system, resulting in and advective and diffusive flux, and biological processes, such as growth and loss. Phytoplankton growth, *g*, depends on nutrient availability, *N(z,t),* and light conditions , *I(z,t)*. They are subjected to a constant natural mortality rate, *m*, due to diseases and aging, and to a grazing mortality, *γ*, by zooplankton. Unlike natural mortality, grazing is not expected to be linearly correlated with phytoplankton concentration, as high phytoplankton concentration can lead to increased grazing rates (Beckmann and Hence, 2007). This density dependence is expressed here with a quadratic term of P. Nutrients, N, are affected by diffusion by not by advection, since bioavailable nutrients are dissolved in the water and are not able to "sink". They are depleted by phytoplankton at the same rate at which phytoplankton are growing and are replenished by a constant linear remineralization rate, *ε*, which encapsulates the microbial processes that are recycling organic matter in the ocean. In this model, the term detritus, *D*, contains both dead phytoplankton and living zooplankton, and is therefore dependent on the grazing and natural mortality of phytoplankton as well as the remineralization by microbes. The governing partial differential equations can be summarized as follows:

(1)

$$\frac{\partial P}{\partial t} = -\frac{\partial J_P}{\partial z} + g(I,N)P - mP - \gamma P^2$$

$$\frac{\partial N}{\partial t} = -\frac{\partial J_N}{\partial z} - g(I,N)P + \varepsilon D$$

$$\frac{\partial D}{\partial t} = -\frac{\partial J_D}{\partial z} + mP + \gamma P^2 - \varepsilon D$$

, where *P(t,z)* is the concentration of phytoplankton, *N(t,z)* is the concentration of nitrogen, *D(t,z)* is the concentration of detritus, *m* is the mortality rate of phytoplankton, *g(I(t,z),N(t,z))* is a function describing the growth rate of phytoplankton, J_P is the total flux of phytoplankton, J_N is the total flux of nutrients, J_D is the total flux of detritus, *ε* is the remineralization rate, *γ* is the grazing rate.

2.2 Spatial discretisation

The model was solved numerically using with the software R x64 version 4.2.2 from 31.10.2022 (Copyright (C) 2022 The R Foundation for Statistical Computing). In order to solve the system of differential equations, a discretisation of either time or space was necessary. In the present study, the water column was divided into discrete units, "grid cells", each being 2.5 m long. Since the total depth of the chosen water column is 100 m, a total of 40 grid cells were created (Figure). The water column z was then modelled as a vector these 40 grid cells, where each depth corresponds to the centre of a given cell. The concentrations of *P*, *N*, and *D* for each given cell were computed.

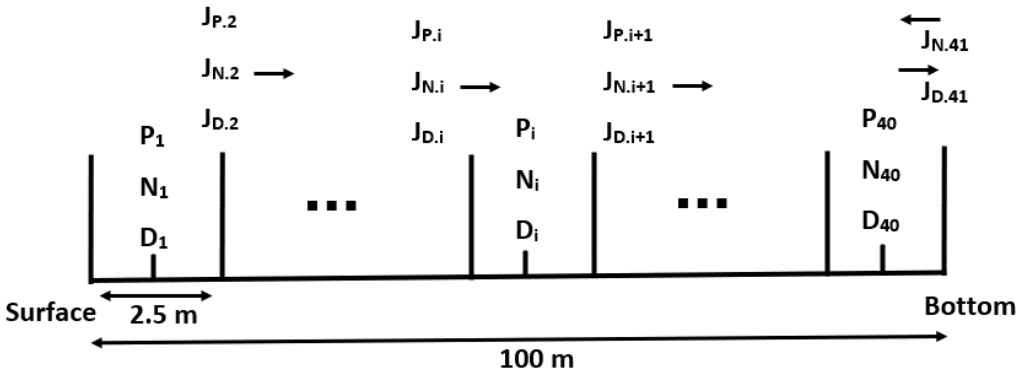

Figure 2: Spatial discretisation.

2.3 Light dependency of phytoplankton growth

The seasonal light variation in the chosen location can be described by the following equation:

(2)

$$season(t) = 1 + \cos\left(\pi + \frac{2\pi}{365}t + \frac{22\pi}{365}\right)$$

, where *t* represents time in days.

This function is used as a multiplier of I_0 (light irradiance at the surface), when the light intensity for time and depth will be computed (see below). The function varies between 0 and 2 and will be equal to 0, i.e., no sunlight, on the 21st of December every year, corresponding to the winter solstice, assuming that there are 365 days in a year. This is ensured by the term $\frac{22\pi}{365}$ added to the period. On the other hand, it will assume a maximum value of 2 on the 172nd day, corresponding to the 21st of June of every year, i.e., on the summer solstice. This should be an accurate reconstruction of light conditions at the border of the Arctic circle, corresponding to latitudes around 66°34'N. The model will run from the 1st of January (day 0) for a variable number of years until a steady state is reached.

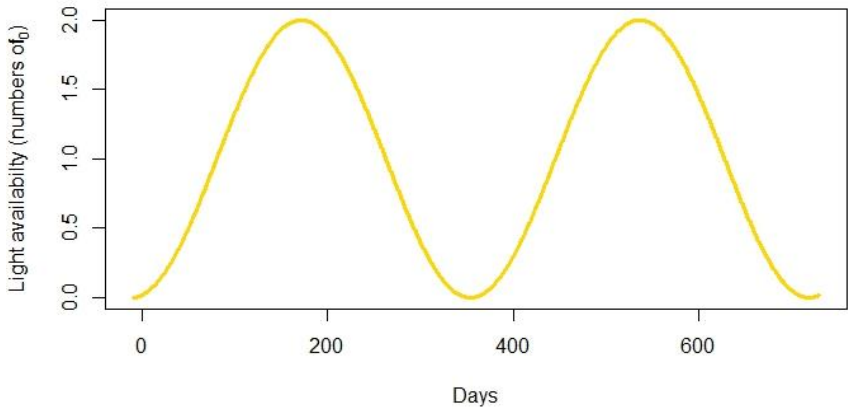

Figure 3: Light availability (in number of I_0, which is the light irradiance at the surface)

In this system, phytoplankton and detritus absorb light incoming from the surface, based on a shading coefficient k_c, and are expected to increase the turbidity of the water. Conversely, nutrients, which are dissolved in the seawater, are not expected to absorb a significant amount of light, compared to

phytoplankton and detritus. The light absorption by phytoplankton and detritus in a specific grid is determined by the concentration of phytoplankton and detritus of the entire column above the grid cell of interest and is given by the following equation:

(3)

$$Q_i = k_c \Delta z \left(\left(\sum_{j=1}^{i-1} P_j \right) + \frac{P_i}{2} + \left(\sum_{j=1}^{i-1} D_j \right) + \frac{D_i}{2} \right)$$

, where Q_i is a measure of the light absorption, k_c is the shading coefficient of detritus and phytoplankton, Δz is the size of the grid cell.

Here, Q_i is a measure of the light absorption by the phytoplankton and detritus present in the water column above the grid cell of interest *i*. The summation parameter j can assume values from 1 to *i*-1, corresponding to all grid cells above the grid cell *i*. The summands $\frac{P_j}{2}$ and $\frac{D_j}{2}$ are present to include the phytoplankton and detritus concentrations present in the upper half of the grid cell *i*. Finally, these equations can then be combined with the Lambert-Beer law to derive the light intensity at each grid cell:

(4)

$$I_i = season \cdot I_0 \cdot \exp\left(-Q_i - k_w z_i\right)$$

, where *I* is the light irradiance for a given depth *i* and at a given time, I_0 is the light irradiance at the surface, k_w is the light absorption coefficient of seawater, and Q_i and *season* are the functions described above.

2.4 Phytoplankton growth

Phytoplankton need both light and nutrients to grow. In this model both light and nutrients limit phytoplankton growth. A type II functional response dependent on nutrients is commonly used for phytoplankton and was therefore used in this model (Beckmann and Hence, 2007; Ryabov et al., 2010). Light limitation was implemented with a different equation that, compared to a type II functional response like the nutrient limitation function, reaches the plateau faster. Liebig's law of the minimum was then implemented, by taking the minimum value between the light and nutrient limitation functions:

(5)

$$g = g_{max} MIN\left(\frac{\alpha I}{\sqrt{{g_{max}}^2 + (\alpha I)^2}}; \frac{N}{N + H_N} \right)$$

, where g_{max} is the maximum growth rate, H_N is the half saturation constant for nutrients and α is the initial slope of the *PI*-curve.

2.5 Diffusive and advective fluxes

The total flux at the boundary between two adjacent grid cells, *i* and *i+1*, is given by the sum of the advective (J_A) and diffusive (J_D) fluxes. The diffusive flux is proportional to the gradient of the

concentration of nutrients, phytoplankton, or detritus (hereafter *N*,*P* and *D* respectively) and its direction is opposite to the gradient. The change of either *N*, *P* or *D* in a given cell *i* is therefore the difference of the flux going in and the flux going out. This can be approximated by the difference in the concentrations of the two grid cells, multiplied by a diffusivity coefficient, D_v. Therefore, the diffusive fluxes for *N*, *P*, and *D* are calculated as follows:

(6)

$$J_{DN.i} = -D_v \frac{N_i - N_{i-1}}{\Delta z}$$

$$J_{DP.i} = -D_v \frac{P_i - P_{i-1}}{\Delta z}$$

$$J_{DD.i} = -D_v \frac{D_i - D_{i-1}}{\Delta z}$$

, where D_v is the diffusivity coefficient.

The advective fluxes transports matter depending on the sinking velocity of the matter itself. This flux tis proportional to the sinking velocity, *u,* and the concentration of matter in the previous (upstream) cell. Both *P* and *D* are particulate matter and are thus subjected to this process with different sinking velocities. On the other hand, *N* is dissolved in the water and it cannot "sink". The advective fluxes of *P* and *D* are therefore calculated as follows:

(7)

$$J_{AP.i} = u_P P_{i-1}$$

$$J_{AD.i} = u_D D_{i-1}$$

, where u_D is the sinking velocity of the detritus and u_P is the sinking velocity of phytoplankton.

2.6 Boundary conditions

At the top of the water column, no *N*, *P*, and *D* are expected to enter the system from the atmosphere. Therefore, the diffusive fluxes and the advective fluxes coming into the 1st grid cell (*i*=1) are equal to 0 for all state variables (no advective fluxes for N):

(8)

$$J_{AP.1} = J_{AD.1} = 0$$

$$J_{DN.i} = J_{DP.i} = J_{DD.i} = 0$$

This does not hold true for the bottom of the water column. Here, *D* sinks into the sediment, where it is buried. Therefore, its advective flux at the lower end of the last grid cell (*n*+1) will not be equal to 0. Living phytoplankton is not expected to sink into the sediment and its advective flux is thus set to 0. The diffusive fluxes for *P* and *D* at the bottom are set to 0 as well since there is not *P* and *D* being diffused in the sediment from the water column or vice versa. The sediment can however release nutrients, *N*, such as nitrogen. Therefore, the concentration of nutrients in the sediment was set to be constant at 30 mmol N and the diffusive flux was calculated based on this concentration:

(9)

$$J_{AP.n+1} = 0$$

$$J_{AD.n+1} = u_D D_{n+1}$$

$$J_{DN.n+1} = -D_v \frac{N_b - N_{n+1}}{\Delta z}$$

$$J_{DD.n+1} = J_{DP.n+1} = 0$$

, where N_b is the concentration of nutrients in the sediment.

2.7 Model parameters

The model parameters were estimated for an oligotrophic ocean ecosystem, characterized by clear water. Numerous model parameters were taken by previous studies (Table 1). Other parameters were estimated based on the location of the system (latitude) and the type of ecosystem. As example, a I_0 of 350 µEinstein was taken from Huisman and Sommeijer (2002), who modelled light-limited environments. Unlike Beckmann and Hence (2007), from where most parameters were taken, in this model *P* and *D* have different sinking velocities. Since living phytoplankton is expected to sink orders of magnitude slower than detritus, the u_P was set to 0.5 m^{-1}. The diffusivity D_v was taken from Beckmann and Hence (2007) but was converted into the units used in this model. Similarly, the parameter α was taken from Beckmann and Hence (2007) but converted to units used in this study. A maximum growth rate of 1.5 d^{-1} was chosen here. For phytoplankton, a growth rate over >1 d^{-1} is common, since these small organisms are very efficient and fast growers. The parameter γ was estimated in Beckmann and Hence (2007) from 0.5 to 2.5 m^3 $mmolN^{-1}$ d^{-1}, however in this model the value had to be adjusted to 0.1 m^3 $mmolN^{-1}$ d^{-1} to ensure the survival of phytoplankton.

Table 1: Symbol, description, unit, and source of the model parameters. (µEinstein corresponds to µmol photons m^{-2} s^{-1}; conc. stands for "concentration")

Symbol	Description	Unit	Value	Source
u_P	Sinking rate of *P*	m d^{-1}	0.5	-
U_D	Sinking rate of *D*	m d^{-1}	15	(Beckmann and Hence, 2007)
D_v	Diffusivity	m^2 d^{-1}	4.32	(Beckmann and Hence, 2007)
Δz	Grid cell size	m	2.5	-
k_c	Shading coefficient of *P* and *D*	m^2 $mmolN^{-1}$	0.05	(Beckmann and Hence, 2007)
k_w	Absorption coefficient of seawater	m-1	0.0375	(Beckmann and Hence, 2007)
I_0	Light irradiance at surface	µEinstein	350	(Huisman and Sommeijer, 2002)
α	Initial slope of *PI*-curve	µ$Einstein^{-1}$ d^{-1}	0.0571	(Beckmann and Hence, 2007)
g_{max}	Maximum growth rate of *P*	d^{-1}	1.5	-
H_N	Half saturation constant for *N*	mmolN m^{-3}	0.3	(Beckmann and Hence, 2007)
m	Mortality of *P*	d^{-1}	0.03	(Beckmann and Hence, 2007)
γ	Grazing mortality of *P*	m^3 $mmolN^{-1}$ d^{-1}	0.1	-
ε	Remineralization coefficient	d^{-1}	0.1	(Beckmann and Hence, 2007)
n	Depth of water column	m	100	-
N_b	Nutrient conc. at the bottom	mmolN m^{-3}	30	-

The model simulations were carried out with a starting concentration of 10 mmol N m^{-3} of phytoplankton (*P*), 30 mmol N m^{-3} of nutrients (*N*), and 0 mmol N m^{-3} of detritus (*D*). The chosen nutrient concentration is the same as the nutrient concentration in the sediments. While these initial conditions may seem a bit large, they will not affect the steady state of the model. They may however affect the time it takes for the model to reach the equilibrium.

3. Results

3.1 Convergence

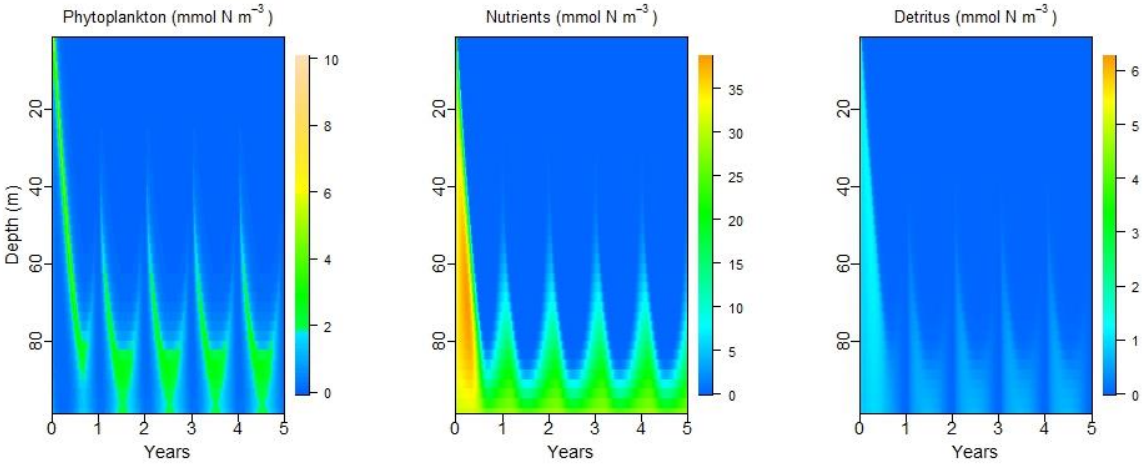

Figure 4: Model simulation over a 5-year period. The phytoplankton (left), nutrient (centre), and detritus (right) concentration reach a steady state after 1 year. From here on a period pattern can be observed.

The model results converge after 1 year since the pattern observed from year 1 to year 2 repeats itself during the following years (Figure 4). The same conclusion can be observed when looking at vertical profiles for a selected variable (Figure 5). If we look at the vertical profile of phytoplankton during the summer solstice, we can notice that it does not significantly change after year 1 (Figure 5). It can therefore be concluded that after 1 year, the system reaches a steady state.

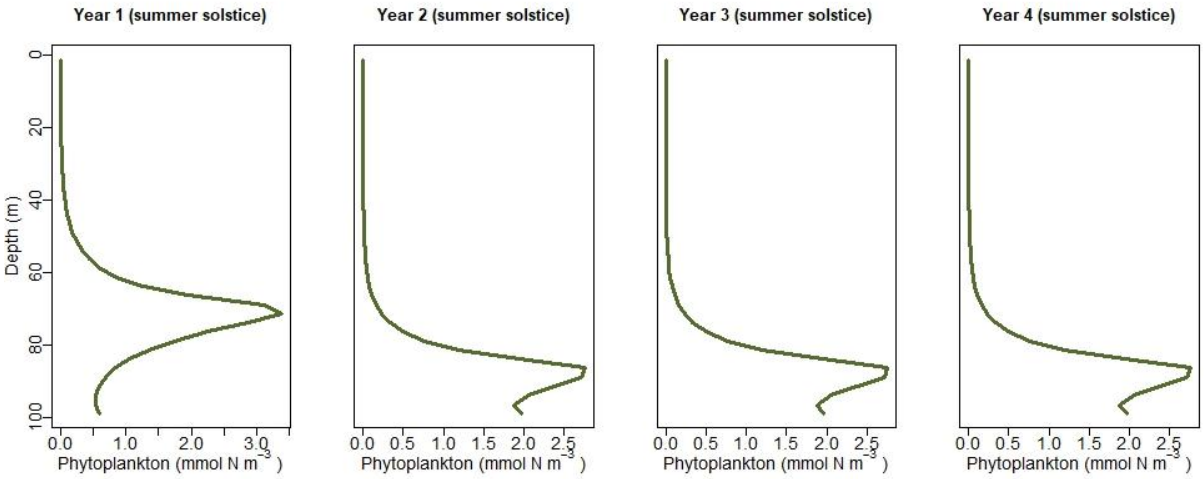

Figure 5: Vertical profiles of phytoplankton concentration in the water column during the summer solstice (the day with the maximum light irradiation) for four different years. The profile does not change from year 2 to year 4.

3.2 Grid sensitivity

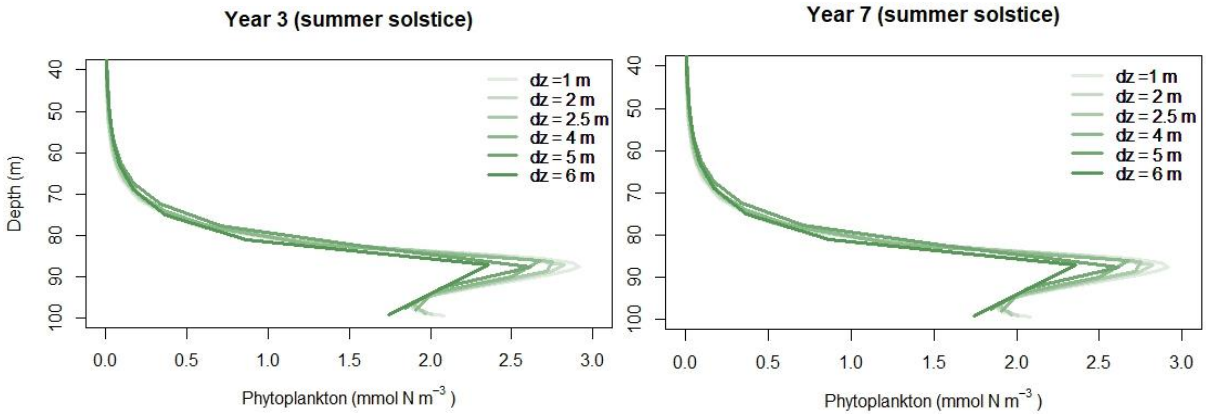

Figure 6: Vertical profile of phytoplankton for 6 different values of the grit size, Δz (m) for the summer solstice after 3 years (left) and after 7 years (right).

When the water 100 m column was divided into grid cells (see Section 2.2) a low spatial resolution of Δz=2.5 m had to be chosen to allow a quick numerical solution of the model. With a higher computational power, a smaller Δz would have been chosen. Therefore, it is necessary to check whether the numerical solution is independent of grid size. The model was therefore run for smaller and larger values of Δz than the used value of 2.5 m (Figure 6). It was not possible to experiment with values of Δz smaller than 1 as the numerical solution of the model would have taken too long. For values of Δz between 1 and 5 m, the numerical solution, in this case the vertical profile of phytoplankton of the summer solstice of the 3rd year, changes minimally. The DCM for Δz=5 m is only approximately 0.4 mmolN m^{-3} lower than for Δz=1 m. On the other hand, when Δz become larger than 4 m, the DCM peak becomes much smaller (difference >0.6 mmolN m^{-3}), making the model results less reliable. It was therefore concluded that a Δz of 2.5 m is a decent resolution for this model.

The same was analysis was done with a model simulation of 7 years to check whether the numerical solution was converged already after 3 years. Since the curves look identical it is expected that the solution is converged in this time span.

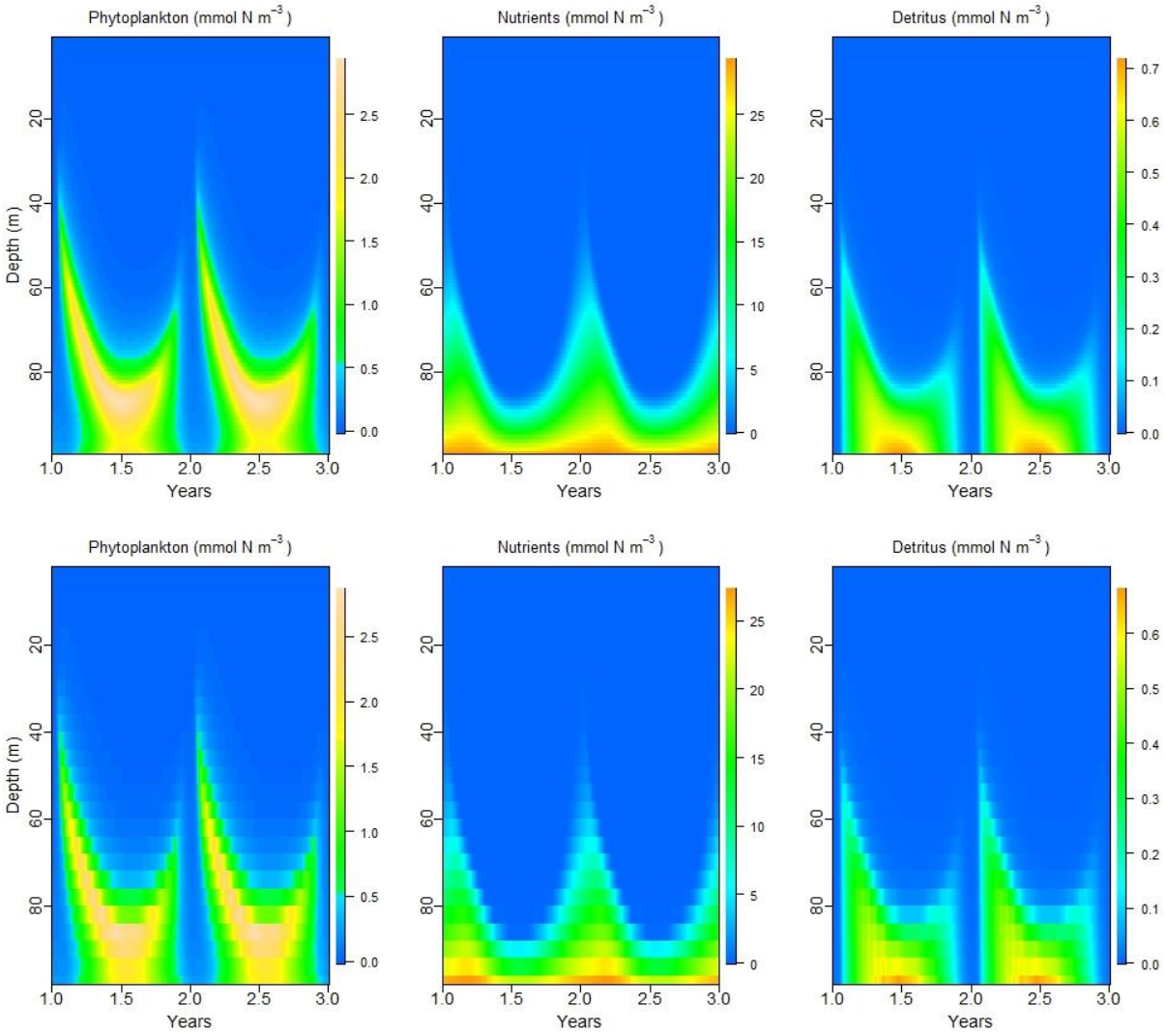

Figure 6: Surface plot showing the steady state solution for Δz=1 m (A) and for Δz=4 m (B). The numerical solutions are virtually identical, suggesting that the solution does not depend on grid size for Δz values between 1 and 4 m.

3.3 Steady-state solution and seasonality

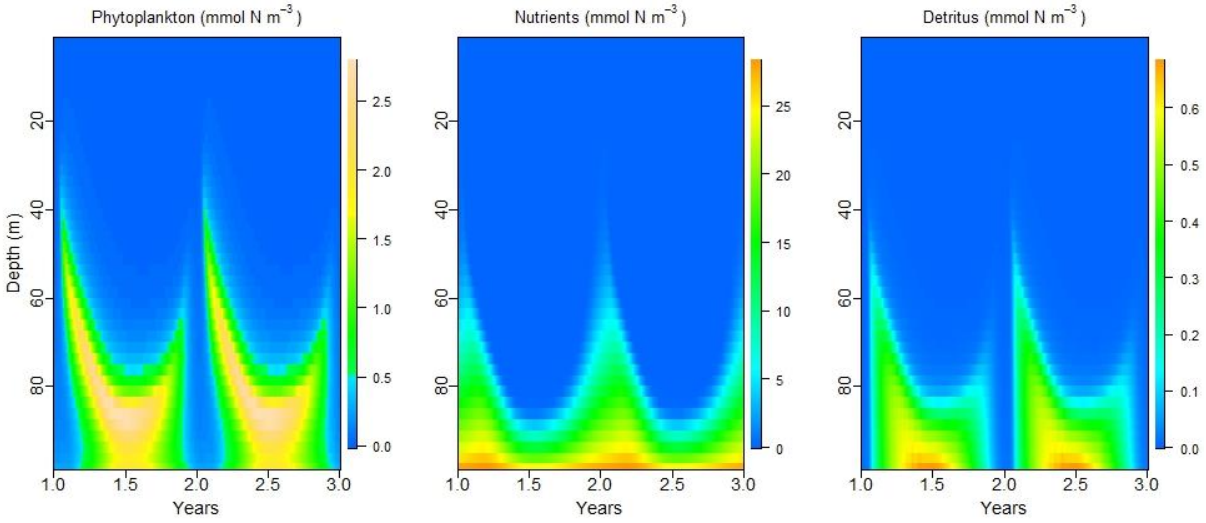

Figure 7: Steady state solution of the model.

The model simulation suggests that the variation in light irradiation during the year generates an annual seasonal pattern in phytoplankton, nutrient, and detritus concentrations (Figure 8 and 9). Not long after the beginning of the year, when light conditions become favourable, phytoplankton start to grow rapidly between 20 and 40 m of depth (Figure 8 and 9 a and b). Simultaneously, an increase in detritus can be observed. The detritus sinks faster than the phytoplankton and accumulates deeper in the water column. This causes an accumulation in nutrients directly below the primary production (Figure 8 and 9 a and b). During the months of the year with the highest light irradiance, around the summer solstice, the bulk of the phytoplankton concentration stabilizes at around 90 m of depth (Figure 8 and 9 c and d). This corresponds to the Deep Chlorophyll Maximum (DCM) that can often be observed in oligotrophic oceanic ecosystems (Beckmann and Hence, 2007). Directly beneath the detritus settles and the nutrients accumulate. Towards the end of the year, the phytoplankton gradually decreases and moves up in the water column. Similarly, the detritus decreases and can be observed further up the water column. As a consequence, the nutrients are transported upwards and redistributed in the water column and at the end of the year, a good amount of nutrients can be observed again at depths from 60 m onwards. This can ensure a new bloom during the spring of the following year (Figure 8 and 9 a and d).

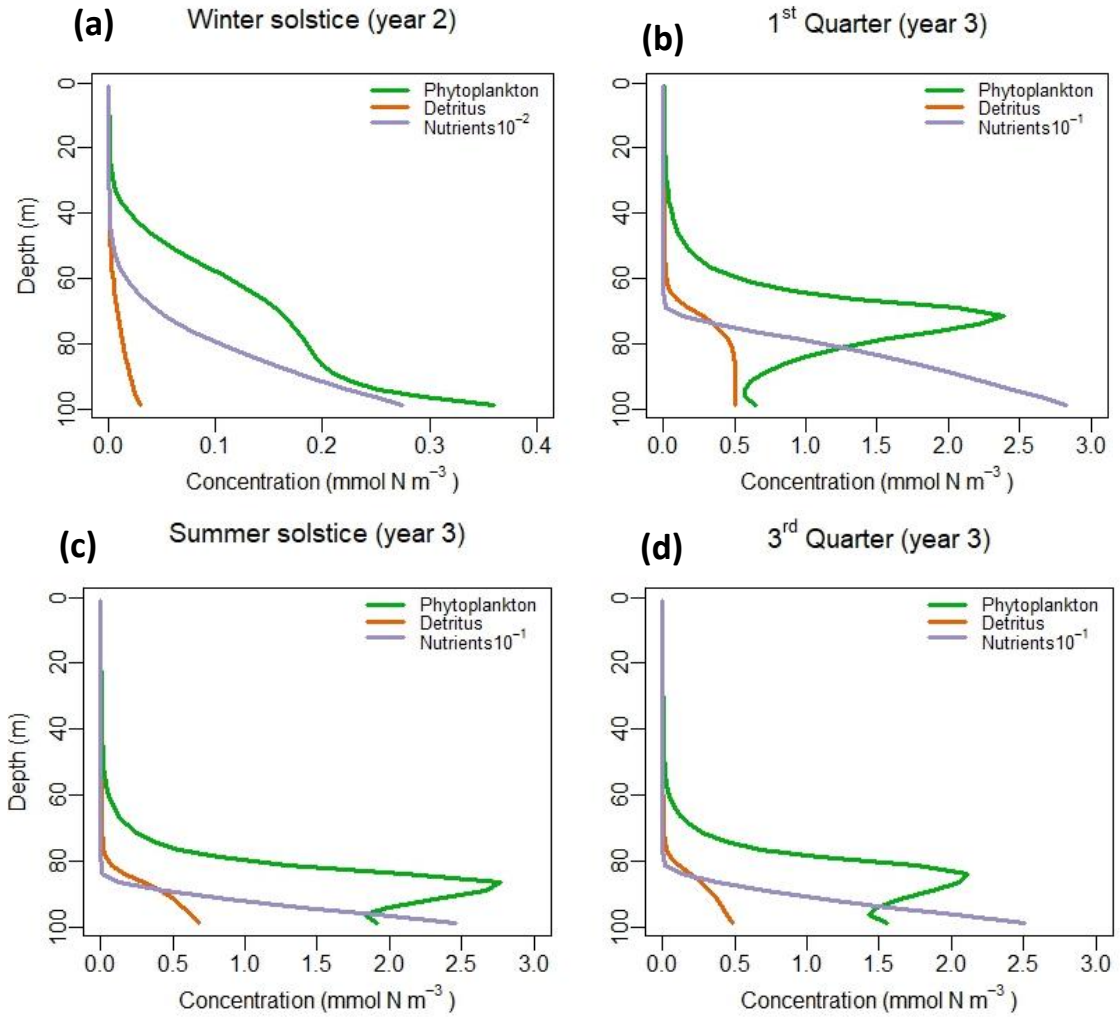

Figure 8: Vertical profiles of phytoplankton (green), nutrients (red), and detritus (blue) for the summer solstice (left) and the winter solstice (right) once the steady state is reached.

3.4 Limitation of phytoplankton growth

The above-mentioned pattern in seasonality can be explained by the phytoplankton growth limitation functions for nutrients and light. Since the winter solstice is defined in this study as the day of the year with no light, no phytoplankton will be able to grow on this day (Figure 9 a). At the start of the year, nutrients can be found relatively high up in the water column (Figure 9 e). Only in the top 30 m nutrients limit phytoplankton growth; below 30 m the limiting factor is light availability, which is low even close to the surface during the winter months. If the minimum value of these two curves is taken at each depth, it can be observed that the highest potential phytoplankton growth rate is found at around 30 m of depth, approximately where the spring bloom can be observed to start (Figure 5; Figure 9 b). During the summer, after the spring phytoplankton bloom has depleted all nutrients in the top 80 m of the water column, nutrient availability is limiting up until 80 m. After 80 m depth, where the nutricline can be found, light becomes the limiting factor. The high light absorption of light between 60 and 80 m is mainly due to the shading of detritus and phytoplankton. If the minimum value of these two curves is taken at each depth, it can be observed that the highest potential phytoplankton growth rate is found at around 90 m of depth, exactly where the summer DCM is observed. During the autumn, it can be noticed that the nutrients become limiting slightly higher up in the water column (Figure 9 d).

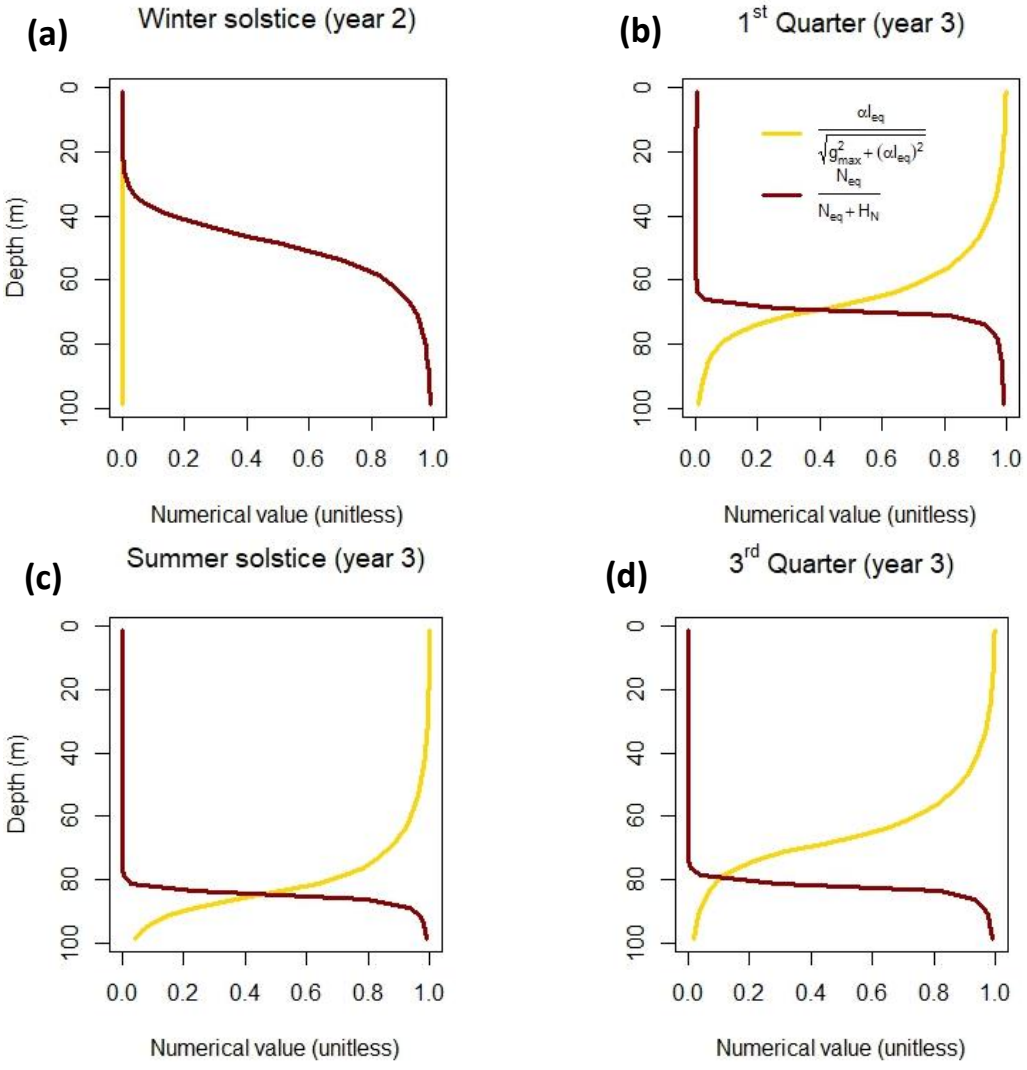

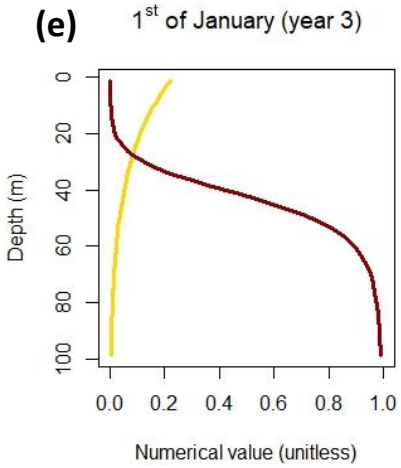

Figure 9: Limitation of phytoplankton growth depending on light (yellow) and nutrients (red) for the summer solstice (left) and the winter solstice (right).

3.5 Sensitivity to D_v and ε

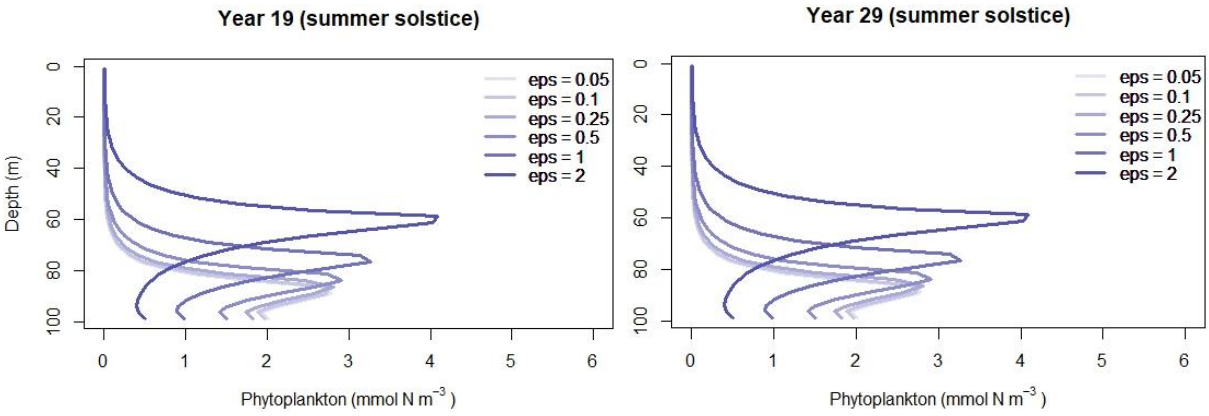

Figure 10: Vertical profile of phytoplankton for 6 different values of the remineralization rate, ε (d^{-1}) for the summer solstice after 3 years (left) and after 7 years (right).

The sensitivity of the model regarding the diffusivity, D_v, and the remineralization rate, ε, was explored. These are important parameters of the model in determining the concentration of nutrients available for phytoplankton growth and are thus expected be important in determining the position and peak magnitude of the DCM.

For an increasing ε, the DCM peak becomes larger, as it would be expected. This observation is caused by the fact that a faster remineralization rate leads to a quicker and more efficient recycling of the nutrients stored in the detritus. These nutrients can be extracted and reused before the detritus sinks too deep in the water column. Furthermore, for an increasing ε, the DCM seems to move further up in the water column. However, care must be taken, since the solution may not yet be fully converged. It took much longer than previous model runs to reach a potential steady state. After 19 years, the vertical profiles of phytoplankton do not seem to change, which is an indication that converged may be reached (Figure 10). This is not an expected result and may only be due to the fact that the solution is not completely converged. Alternatively, this result could be explained by the fact that the detritus is remineralized quickly enough for the diffusive flux to transport the new nutrients further up in the water column.

As D_v increases, the DCM moves further up in the water column. This is expected since the diffusivity determines how much the nutrients are diffused from the deep layer, where they are abundant due to dissolution from the sediment to the upper layers, where light is abundant. Interestingly, the magnitude of the DCM peak does not seem to be strongly affected by D_v. This was not expected, since higher values of D_v should bring nutrients higher up in the water column where the light conditions are more favourable for phytoplankton growth, therefore leading to larger DCM. Moreover, since the curves in the plots for 3- and 7-year modelling are virtually identical, it can be concluded that the solutions are converged.

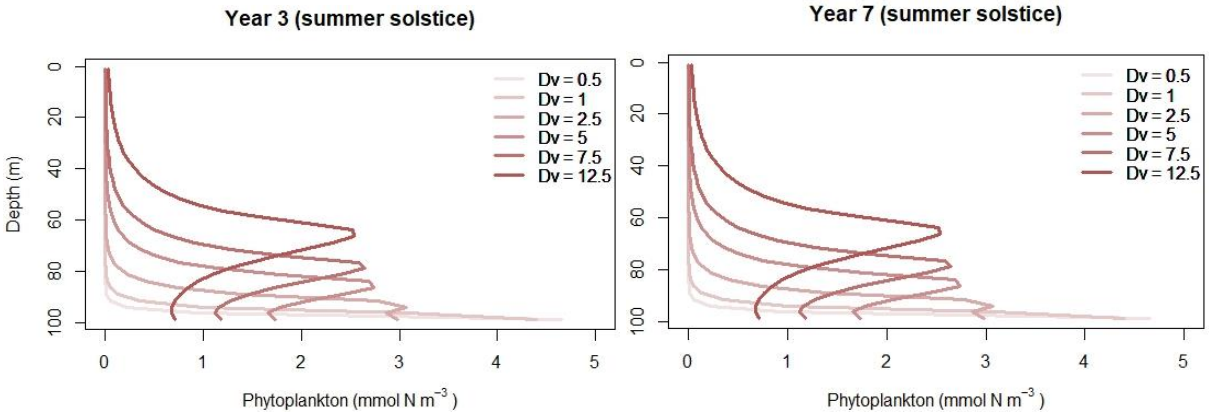

Figure 11: Vertical profile of phytoplankton for 6 different values of the diffusivity coefficient, D_v (m^2 d^{-1}) for the summer solstice after 3 years (left) and after 7 years (right).

4. Discussion and conclusion

While the model used in this study represents an extremely simplified version of the real oceanic environment it can provide useful insight in the mechanisms controlling the DCM in the Arctic Ocean. Moreover, the steady state numerical solution given by the model is surprisingly similar to real-world observation. The DCM in oligotrophic ocean system tends to be located at the upper boundary of the nutricline (Beckmann and Hence, 2007; Figure 8 and 9). Simulation run with this model show the same pattern for an oligotrophic Arctic Ocean.

The model was used to investigate the relevance of two parameters, namely the remineralization rate, ε, and the diffusivity coefficient, D_v, that control the distribution on nutrients in the water column. It was concluded that a higher ε generates a larger DCM, via a quicker and more efficient remineralization of the detritus. Furthermore, a larger ε was also found to potentially move the DCM further up in the water column. However, care must be taken when interpreting this result as the model took longer to reach an apparent convergence and it may not have reached convergence. Similarly, higher D_v values were shown to lead to shallower DCM, which can be explained by a stronger upwards diffusion of nutrients.

Finally, the model was shown to be independent of grid size, for grid cell smaller than 5 m. This allows the model to run fast and requires low computational power. In addition, the model was found to converge quickly, even with starting conditions that were far from the steady state concentrations.

6. References

Beckmann, A. and Hense, I. (2007). Beneath the surface: Characteristics of oceanic ecosystems under weak mixing conditions – A theoretical investigation. *Progress in Oceanography*, 75(4), pp.771–796.

Huisman, J. and Sommeijer, B. (2002). Population dynamics of sinking phytoplankton in light-limited environments: simulation techniques and critical parameters. *Journal of Sea Research*, 48(2), pp.83–96.

Ryabov, A.B., Rudolf, L. and Blasius, B. (2010). Vertical distribution and composition of phytoplankton under the influence of an upper mixed layer. *Journal of Theoretical Biology*, 263(1), pp.120–133.

5. R code on github

Link for the repository: https://github.com/Giacks/NPD.git

Comments:

- week5seasonality4.R: model and the main plots
- dzzgritsensitivity.R: code for the grid sensitivity plots
- dvsensitivity.R: code for the diffusivity sensitivity plots
- remineralizationsensitivity.R: code for the remineralization rate sensitivity plot